Stable RAGE-Heparan Sulfate Complexes Are Essential for Signal Transduction

Ding Xu,*[,†] Jeffrey H. Young,[†] Juno M. Krahn,[‡] Danyin Song,[†] Kevin D. Corbett,[§] Walter J. Chazin,[‖] Lars C. Pedersen,[‡] and Jeffrey D. Esko*[,†]

[†]Department of Cellular and Molecular Medicine, Glycobiology Research and Training Center, University of California, San Diego, La Jolla, California 92093, United States

[‡]Laboratory of Structural Biology, National Institute of Environmental Health Sciences, National Institutes of Health, Research Triangle Park, North Carolina 27709, United States

[§]Ludwig Institute for Cancer Research and Department of Cellular and Molecular Medicine, University of California, San Diego, La Jolla, California 92093, United States

[‖]Departments of Biochemistry and Chemistry, Center for Structural Biology, Vanderbilt University, Nashville, Tennessee 37232, United States

S *Supporting Information*

ABSTRACT: RAGE (Receptor for Advanced Glycation End-Products) has emerged as a major receptor that mediates vascular inflammation. Signaling through RAGE by damage-associated molecular pattern molecules often leads to uncontrolled inflammation that exacerbates the impact of the underlying disease. Oligomerization of RAGE is believed to play an essential role in signal transduction, but the molecular mechanism of oligomerization remains elusive. Here we report that RAGE activation of $Erk_{1/2}$ phosphorylation on endothelial

cells in response to a number of ligands depends on a mechanism that involves heparan sulfate-induced hexamerization of the RAGE extracellular domain. Structural studies of the extracellular V-C1 domain-dodecasaccharide complex by X-ray diffraction and small-angle X-ray scattering revealed that the hexamer consists of a trimer of dimers, with a stoichiometry of 2:1 RAGE:dodecasaccharide. Mutagenesis studies mapped the heparan sulfate binding site and the interfacial surface between the monomers and demonstrated that electrostatic interactions with heparan sulfate and intermonomer hydrophobic interactions work in concert to stabilize the dimer. The importance of oligomerization was demonstrated by inhibition of signaling with a new epitope-defined monoclonal antibody that specifically targets oligomerization. These findings indicate that RAGE-heparan sulfate oligomeric complexes are essential for signaling and that interfering with RAGE oligomerization might be of therapeutic value.
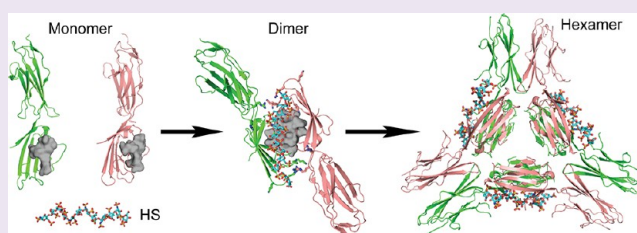
The Receptor for Advanced Glycation End-Products (RAGE) is a promiscuous pattern recognition receptor that interacts with a variety of ligands. RAGE was first discovered as the receptor for advanced glycation end-products (AGE) generated by the Amadori rearrangement of non-enzymatically glycated proteins.[1] Additional ligands include many damage-associated molecular pattern proteins such as S100 proteins and High Mobility Group protein B1 (HMGB1) that are released from the nucleus or cytoplasm in response to inflammation or cellular necrosis.[2,3] Activation of RAGE by its ligands often leads to prolonged inflammation that exacerbates tissue damage in many disease settings, including diabetes, atherosclerosis, multiple sclerosis, ischemic-reperfusion injury and sepsis.[4−8] Therefore, there is great interest in developing agents to antagonize RAGE signaling as a way to suppress uncontrolled inflammation.

RAGE is a multidomain protein consisting of three extracellular immunoglobulin domains (V-C1-C2, also known as sRAGE), a single transmembrane domain, and a short

cytoplasmic tail.[9] The two most N-terminal immunoglobulin domains, V and C1, are responsible for most if not all ligand binding.[10−13] The short cytoplasmic tail lacks intrinsic kinase activity but serves an essential role in signal transduction by recruiting adaptor proteins, such as Diaphanous-1 and Toll-Interleukin 1 Receptor Domain containing Adaptor Protein (TIRAP), or the extracellular signal-regulated kinase Erk1.[14−16] RAGE oligomerization has been observed *in situ* at the cell surface using fluorescence resonance energy transfer and chemical cross-linking.[17,18] Immunoprecipitation and *in vitro* binding assays further support that RAGE can self-associate.[10,12,18,19] Moreover, disrupting oligomerization of endogenous RAGE with sRAGE results in greatly reduced mitogen-activated protein kinase phosphorylation and nuclear factor NF-κB activation, suggesting that targeting RAGE oligomeriza-

tion might have therapeutic potential.[18] Key questions that remain unanswered concern the mechanism of RAGE oligomerization and the organization of the oligomers.

Here we report that heparan sulfate is an integral part of the functional RAGE signaling complex and functions by promoting RAGE oligomerization. We show that dodecasaccharides derived from heparin, a highly sulfated form of heparan sulfate, support formation of a stable RAGE hexamer, with a stoichiometry of 2:1 RAGE:oligosaccharide. We further present the crystal structure of the RAGE hexamer in complex with dodecasaccharides, which is arranged as a trimer of dimers. The solution structure of RAGE hexamer was also determined by small-angle X-ray scattering (SAXS) and shows a high degree of agreement with the crystal structure. Finally, these structural insights led to the successful identification of an epitope-defined monoclonal antibody that inhibits RAGE signaling by hindering RAGE oligomerization.

RESULTS AND DISCUSSION

Endothelial Heparan Sulfate Is Essential for RAGE Signaling. RAGE is a transmembrane receptor that binds many damage-associated molecular pattern proteins. Previous studies showed that RAGE on the cell surface exists as an oligomer of unknown stoichiometry,[17,18] but a stable RAGE oligomer has not been reported to form in vitro, which greatly hinders biophysical characterization of RAGE oligomerization. Recently, we showed that RAGE exists in a complex with heparan sulfate,[20] a ubiquitous polysaccharide found covalently linked to membrane and matrix proteoglycans. To gain better insight into the role that heparan sulfate plays in receptor architecture and function, we first tested a variety of ligands that activate RAGE. Some of these ligands bind to heparan sulfate (HMGB1, S100A8/A9 and S100A12), whereas others do not (S100b, AGE-BSA).[21−23] Nevertheless, RAGE signaling by all five ligands depends on heparan sulfate, as measured by the loss of $Erk_{1/2}$ phosphorylation after removal of cell surface heparan sulfate (Figure 1). $Erk_{1/2}$ phosphorylation was chosen as the
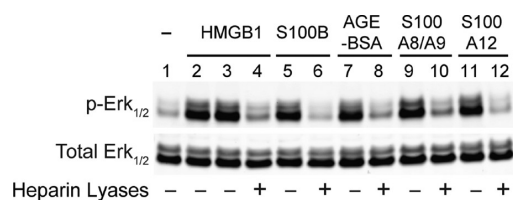

Figure 1. Endothelial heparan sulfate is required for RAGE signaling. $Erk_{1/2}$ phosphorylation of primary human endothelial cells was measured by immunoblotting before (lane 1) and after stimulation by RAGE ligands (lanes 2−12). In lane 2, endothelial cells were stimulated for 15 min with a mutated form of HMGB1 that does not bind heparan sulfate. Cells were stimulated with wild-type HMGB1 (lanes 3 and 4), S100B (lanes 5 and 6), AGE-BSA (lanes 7 and 8), S100A8/A9 (lanes 9 and 10) or S100A12 (lanes 11 and 12). Selected samples were treated with heparin lyases I, II and III for 15 min prior to adding ligand as indicated.

readout of RAGE signaling because it is associated with RAGE activation in endothelial cells.[7,20] Thus, the requirement for heparan sulfate for signaling appears to be an intrinsic property of RAGE.

Heparin-Derived Oligosaccharide Induces a Stable RAGE Oligomer. To test if heparan sulfate promotes RAGE oligomerization, we mixed recombinant sRAGE (V-C1-C2

domains) with heparin-derived oligosaccharides of defined size and examined RAGE oligomerization by size exclusion chromatography (SEC). Heparin is related in structure to heparan sulfate and thus mimics the behavior of heparan sulfate in most systems. By itself, sRAGE eluted from the column as a monomer, with an apparent molecular mass larger than its predicted mass (~41 kDa vs 32 kDa), presumably due to its elongated shape.[9,10] However, when we mixed sRAGE with heparin-derived dodecasaccharide (dp12), sRAGE eluted as a single peak of ~200 kDa (Figure 2a). The formation of this oligomer has a strict dependence on the length of the oligosaccharide, as exemplified by a total lack of oligomerization by heparin decasaccharide (dp10) (Figure 2a). We also found that V-C1 domains were sufficient to support the formation of a stable oligomer (Supplemental Figure 1a).

We next examined the stoichiometry of the sRAGE/oligosaccharide complex by isothermal titration calorimetry (ITC). Fitting of the thermogram for titration of the dodecasaccharide into sRAGE yielded a dissociation constant (K_d) of 114 ± 18 nM and a stoichiometry of 0.49 ± 0.01 (Figure 2b), suggesting the stoichiometry of the oligomeric complex is two RAGE molecules to one oligosaccharide. Using multiple-angle light scattering (MALS) coupled with SEC, we determined the complex has a molecular mass of 196 ± 5 kDa, very close to the predicted molecular mass of an sRAGE hexamer plus 3 oligosaccharides (202 kDa, Supplemental Figure 1b).

Location of the Heparan Sulfate-Binding Site of RAGE. To identify the amino acid residues that are responsible for binding of RAGE to heparan sulfate, a systematic site-directed mutagenesis study of the 22 conserved lysine and arginine residues in V-C1 was performed (Supplemental Figure 2). Alanine substitution mutants of seven residues showed greatly reduced binding to heparin-Sepharose, displaying a reduction of 50−110 mM in salt concentration required for elution (Supplemental Table 1). Among the residues identified in this way, five were located in the V domain (K39, K43, K44, R104 and K107) and two were located in the C1 domain (R216 and R218, Figure 2c).

We also found that these mutants showed greatly reduced binding to endothelial heparan sulfate in solution, and the effect was especially dramatic with double mutants (Figure 2d). However, these mutants bound the ligand HMGB1 with a K_d of 8−13 nM (10 nM for wild-type RAGE) and to S100b with a K_d of 63−90 nM (83 nM for wild-type RAGE) (Supplemental Table 2). The preservation of HMGB1 and S100b binding affinity suggested that these ligands and heparan sulfate interact with separate surfaces of RAGE. We also found that all heparan sulfate-binding mutants displayed substantially reduced hexamer formation (70−100% reduction compared to wild-type RAGE) when mixed with oligosaccharide (Supplemental Figure 3).

Heparan Sulfate Stabilizes a Hydrophobic Dimeric Interface of RAGE. Examination of the crystal structures of the monomeric RAGE V-C1 domain (PDB ids: 3CJJ and 3O3U) revealed a hydrophobic patch (P33, V35, L36, V78, L79, P80, F85, L86, and P87) that is involved in crystal packing between two molecules (Figure 3a). To test if these residues mediate oligomerization, we prepared three mutants in the center of the hydrophobic patch (V35A, V78A-L79A, F85A-L86A). Remarkably, all three mutants showed severe defects in hexamerization. The single mutation, V35A, supported partial hexamer formation when mixed with oligosaccharide, but the
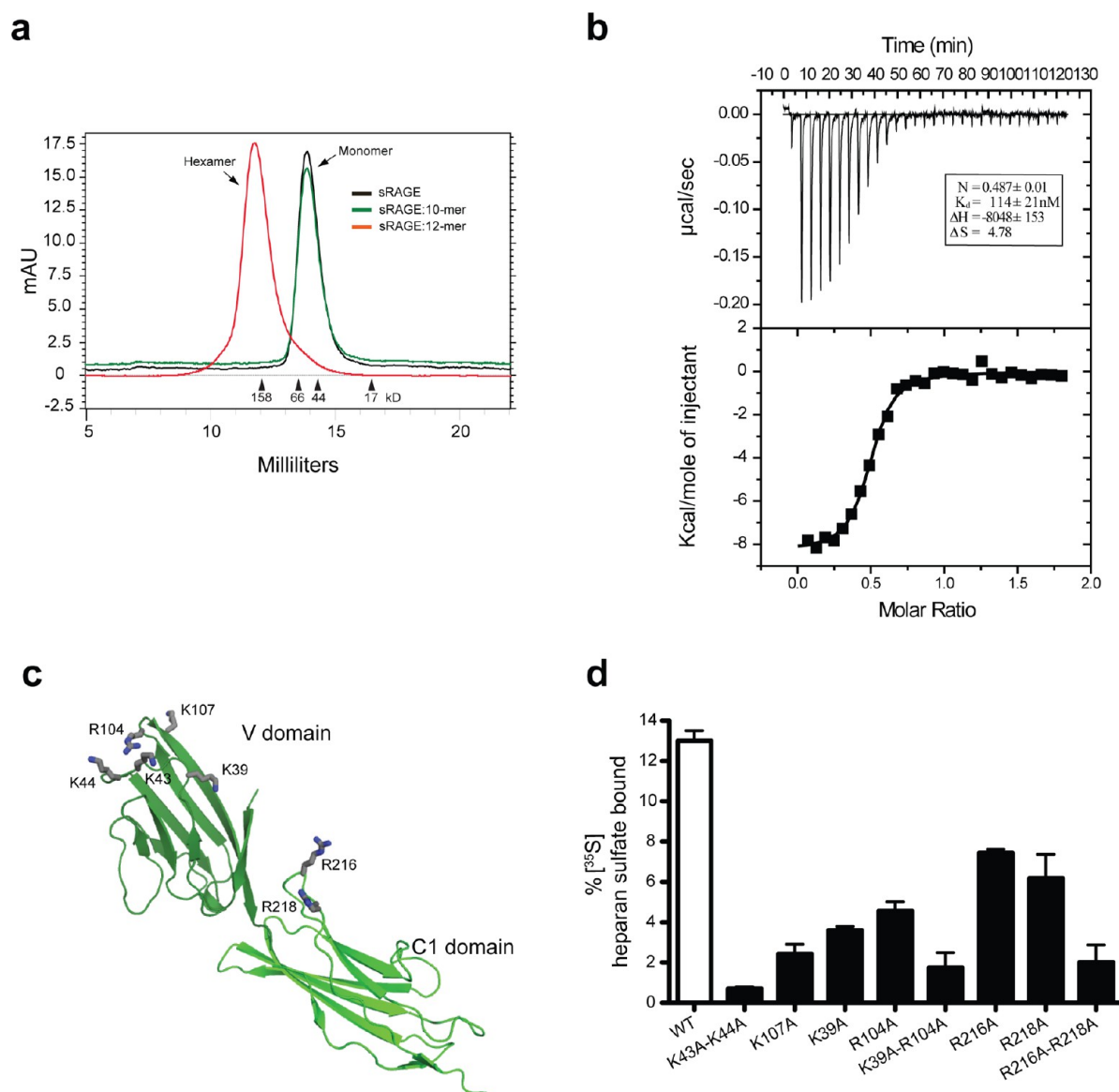
a

b

c

d

Figure 2. Heparin-derived dodecasaccharides induce a stable oligomer of RAGE. (a) Mixtures of sRAGE and heparin-derived decasaccharides or dodecasaccharides were resolved by SEC. (b) Binding of dodecasaccharides was monitored by isothermal calorimetry by titrating sRAGE with dodecasaccharide. (c) Cartoon representation of RAGE V-C1 domain (PDB id: 3CJJ). Amino residues demonstrated to interact with heparan sulfate are shown in stick representation (gray). (d) Binding of wild-type and various RAGE mutants to ^{35}S-labeled endothelial heparan sulfate as determined by filter binding assay ($n = 3$, error bars represent the standard deviation). The extent of binding was quantified by dividing the counts retained by the membrane by the total input counts.

majority of the protein eluted as a broad peak that overlaps with the elution position of the monomer, suggesting that the oligomer was destabilized (Figure 3b). The effect was more pronounced with the two double mutants, V78A-L79A and F85A-L86A, which eluted in SEC exclusively as a broad peak (Figure 3b). MALS analysis of the V78A-L79A mutant suggested that the broad peak contained mostly species with molecular weights in the range of 32−70 kD, consistent with the idea of a monomer/dimer equilibrium (Supplemental Figure 1b).

All three oligomerization mutants showed wild-type level of binding to both HMGB1 and S100b (Supplemental Table 2) and eluted from heparin-Sepharose at a similar salt concentration as for wild-type RAGE (Supplemental Table 1). These findings suggested that the mutants probably maintain wild-type-like folding and that the defects in hexamerization most

likely arose due to destabilized hydrophobic interactions between subunits. On the basis of the cumulative results, we propose that the basic building block of RAGE oligomers is a dimer stabilized by the identified hydrophobic patch.

Examination of the dimer structure (extracted from 3CJJ) showed that two separate heparin binding sites from each subunit converge into a large positively charged cleft that would accommodate a negatively charged heparan sulfate oligosaccharide (Figure 3c). Therefore, it seemed likely that heparan sulfate might function to stabilize the RAGE dimer. Thus, we proposed that heparan sulfate binding and the protein−protein hydrophobic interaction are energetically coupled and that both contribute to the formation of a stable dimer. If this model were correct, one would expect that alanine mutants of the hydrophobic patch, which decrease dimer formation, would decrease the binding affinity of RAGE to heparan sulfate. We
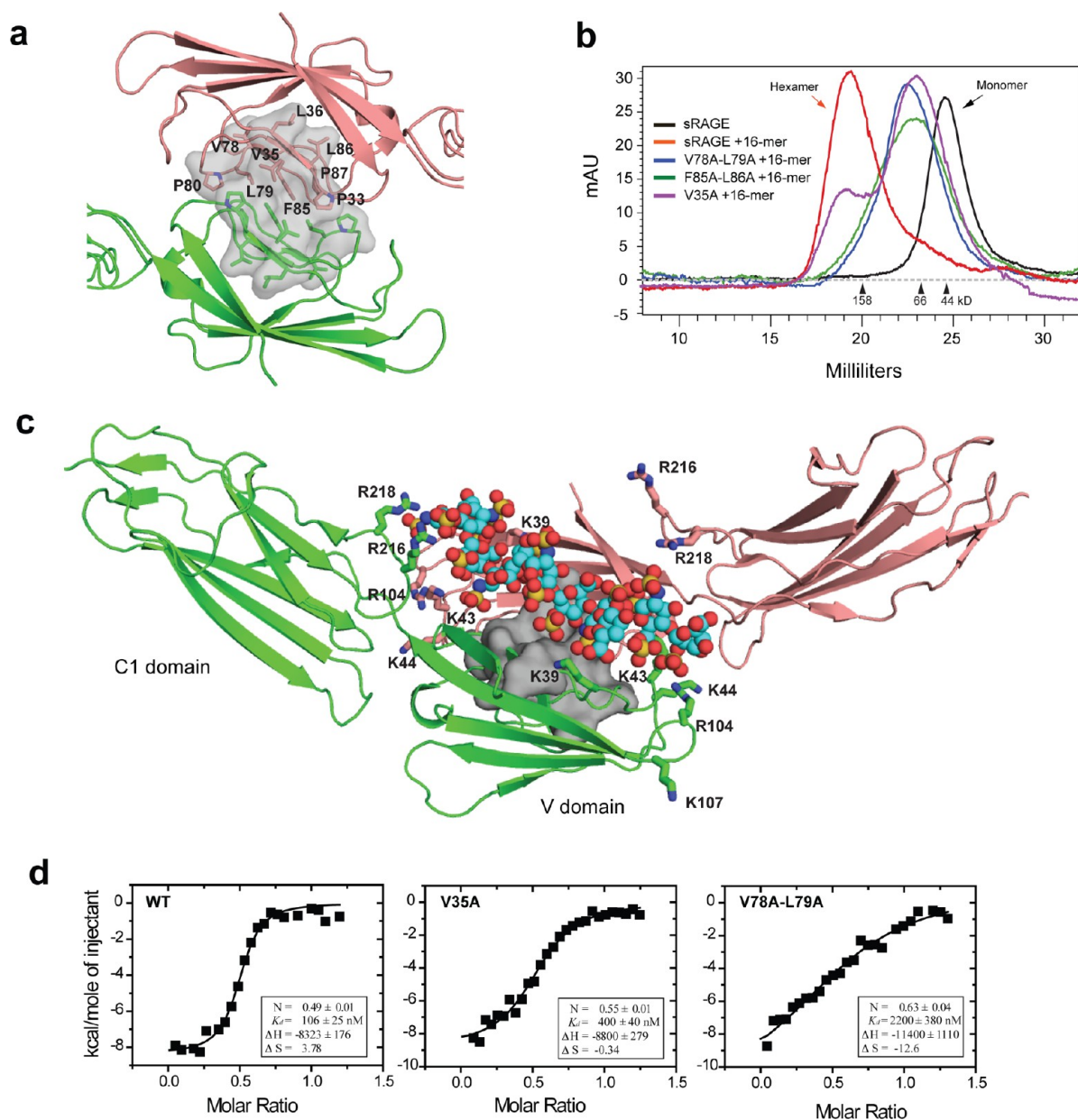
Figure 3. A hydrophobic dimeric interface is stabilized by heparin. (a) Cartoon diagram of the V–C1 dimer (salmon and green) showing the proposed dimeric interface (gray surface) deduced from the crystal structure of hRAGE V–C1 (PDB id: 3CJJ). The relevant hydrophobic residues are shown in stick representation. (b) Mutants of sRAGE were incubated with oligosaccharide at 1:1 molar ratio, and the mixtures were resolved by SEC. (c) The proposed heparan sulfate binding cleft of the dimer. Monomers are shown in green or salmon. Amino acid residues that bind to heparan sulfate are shown in stick representation on the corresponding monomer. A space-filling model of the dodecasaccharide is modeled into the binding cleft (carbon in cyan, oxygen in red, nitrogen in blue, and sulfate in yellow). The hydrophobic interface between the dimers is represented as a gray molecular surface. (d) Binding of dodecasaccharide to wild-type, V35A or V78A-L79A RAGE V–C1 domain was assessed by isothermal calorimetry.

tested this idea by measuring binding of V35A and V78A-L79A mutants to oligosaccharide by ITC. As predicted by the model, V35A, which has a moderate effect on oligomerization, showed 4-fold lower affinity for dodecasaccharide compared to that of wild-type RAGE (400 ± 40 vs 106 ± 25 nM, Figure 3d). In comparison, V78A-L79A displayed a 20-fold lower affinity for dodecasaccharide compared to wild-type (2200 ± 380 vs 106 ± 25 nM, Figure 3d). The stoichiometry of binding of RAGE to dodecasaccharide also deviated from the value of 0.5 observed for wild-type RAGE, giving values of 0.55 and 0.64 for V35A and V78A-L79A, respectively. These findings support the idea

that dimer formation creates the optimal surface for binding to heparan sulfate.

Crystal Structure of mRAGE in Presence of Oligosaccharide. To obtain deeper insight into the oligomerization of RAGE, mouse RAGE V–C1 (mV–C1) was crystallized in complex with dodecasaccharide. The structure was determined at a resolution of 3.5 Å (Figure 4a and Supplemental Figure 4) in space group $P4_132$ with one molecule of mV–C1 in the asymmetric unit (Supplemental Table 3). Lattice packing revealed dimeric interactions between symmetry related V domains similar to that seen in the lattice packing of human RAGE V–C1 (hV–C1, PDB id: 3CJJ). The same dimeric
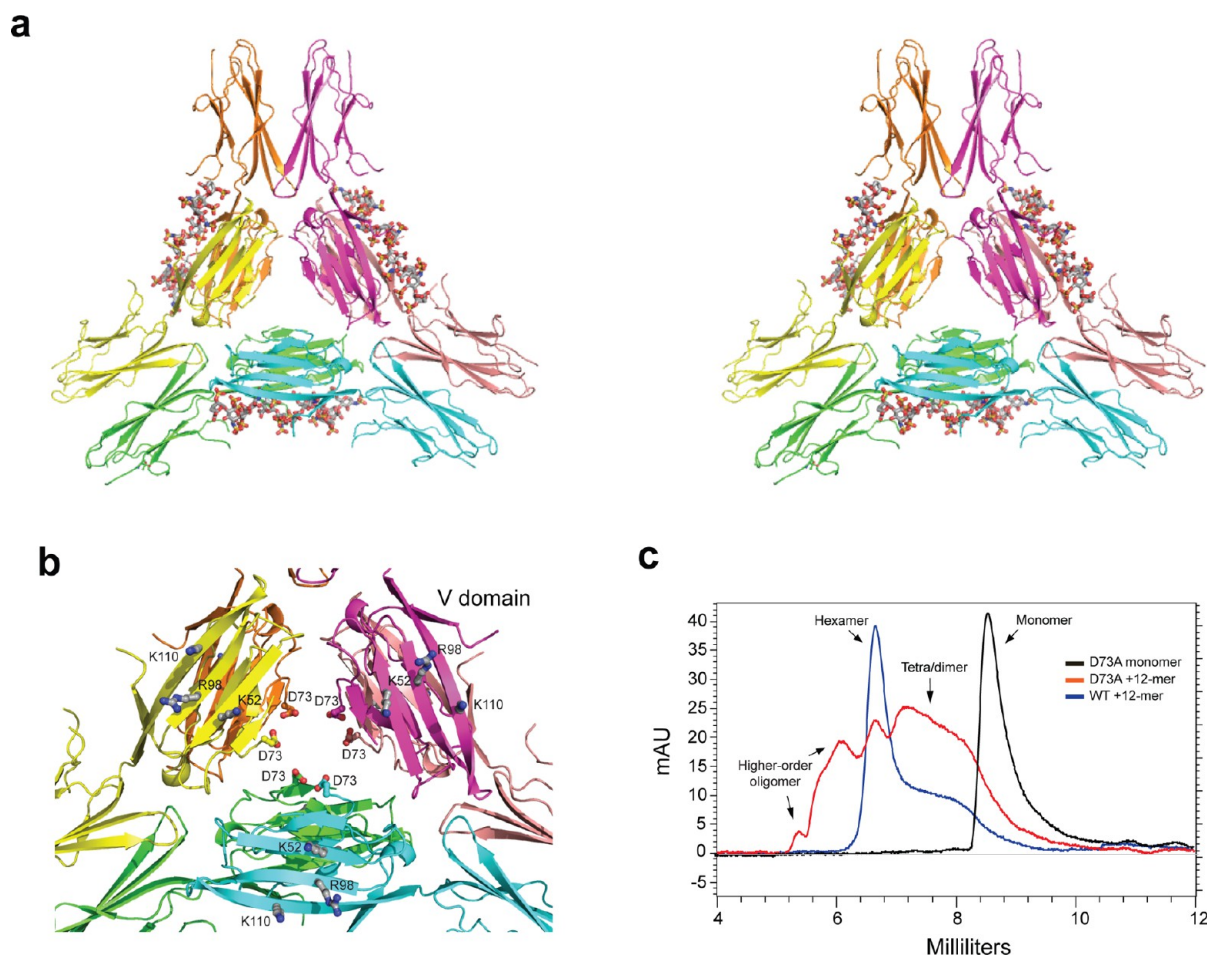
Figure 4. Crystal structure of the RAGE hexamer. (a) Stereo view of the cartoon representation of the crystal structure of the hexameric mRAGE V-C1 domain. The three dimers are colored in green and cyan, yellow and orange, and salmon and magenta, respectively. Dodecasaccharides (in sticks) were modeled into the heparan sulfate binding clefts based on the observed sugar density in the crystal structure. The C-terminal strands, involved in the strand-swap, from neighboring molecules in the crystal are displayed to give a canonical view of the C1 domains. (b) The central part of the hexamer consisting of the V-domains is shown. Residues involved in ligand binding (K52, R98, and K110) are shown as ball and stick model and are located at the surface of the hexamer. The aspartic acids at position 73 of each monomer are oriented inward at the core of the hexamer. (c) D73A mutant or wild-type sRAGE were incubated with oligosaccharide at 2:1 molar ratio and resolved by SEC.

interactions were also present in recently deposited structures of hV-C1 in the presence of DNA (PDB ids: 3S58 and 3S59). The overall fold of mV-C1 closely resembles that of hV-C1 with an RMSD of 0.98 Å over 176 residues. One difference exists: residues P213–R228 of the terminal strand of the C1 domain form a strand swap with a neighboring hexamer in the mV-C1 crystal lattice. In our structure, three dimers come together to form a hexamer with the V domains situated in the center forming a hub and the C1 domains extending outward like six spokes resembling a wheel. This arrangement differs from crystal packing in previously reported V-C1 structures obtained in the absence of heparin.

Although the electron density maps reveal no clear density for a bound dodecasaccharide, there are regions of discontinuous difference density within the proposed heparan sulfate binding cleft (Supplemental Figure 5a). The absence of clearly defined density suggests the dodecasaccharide is bound heterogeneously to V-C1. Interestingly, superposition of the DNA bound hV-C1 structure (PDB id: 3S59) with the crystallographic dimer of mV-C1 reveals that many residues that make contact with the DNA (K39, K43, K107, R216, and R218) are very near the regions of positive difference density in the mV-C1 structure, supporting their role in dodecasaccharide

binding (Supplemental Figure 5b). In the DNA bound crystal structure there is a gap of ∼20 Å and four base pairs across the dimerization interface where there are no hydrogen bond interactions with the DNA. The lack of interactions in this region could contribute to the disorder of the less rigid polysaccharide to mV-C1.

The crystal structure of the hexameric complex is consistent with previous RAGE ligand binding studies in that the proposed S100b, AGE and lysophosphatidic acid binding surface, which includes K52, R98 and K110, is exposed to solvent (Figure 4b).[10,13,24] The architecture of the hexamer indicates that the three dimers are tethered together by interacting with each other within the core of the hexamer. Unfortunately, the majority of a key loop ([65]SPQGGG-PWDS[74]) that is centrally located at the interface is disordered. The conformations of this loop are different among three crystal structures of isolated RAGE V-C1 (3CJJ, 3S59 and 3O3U), which suggests that the loop is flexible.[25] The loop is presumably involved in interdimer interactions. A conserved D73 residue (D72 in mouse) is located at the end of the disordered loop (Figure 4b). The alanine mutant of this residue was detrimental to formation of the hexamer (Figure 4c), consistent with the possible role of D73 as a hexamer stabilizer.
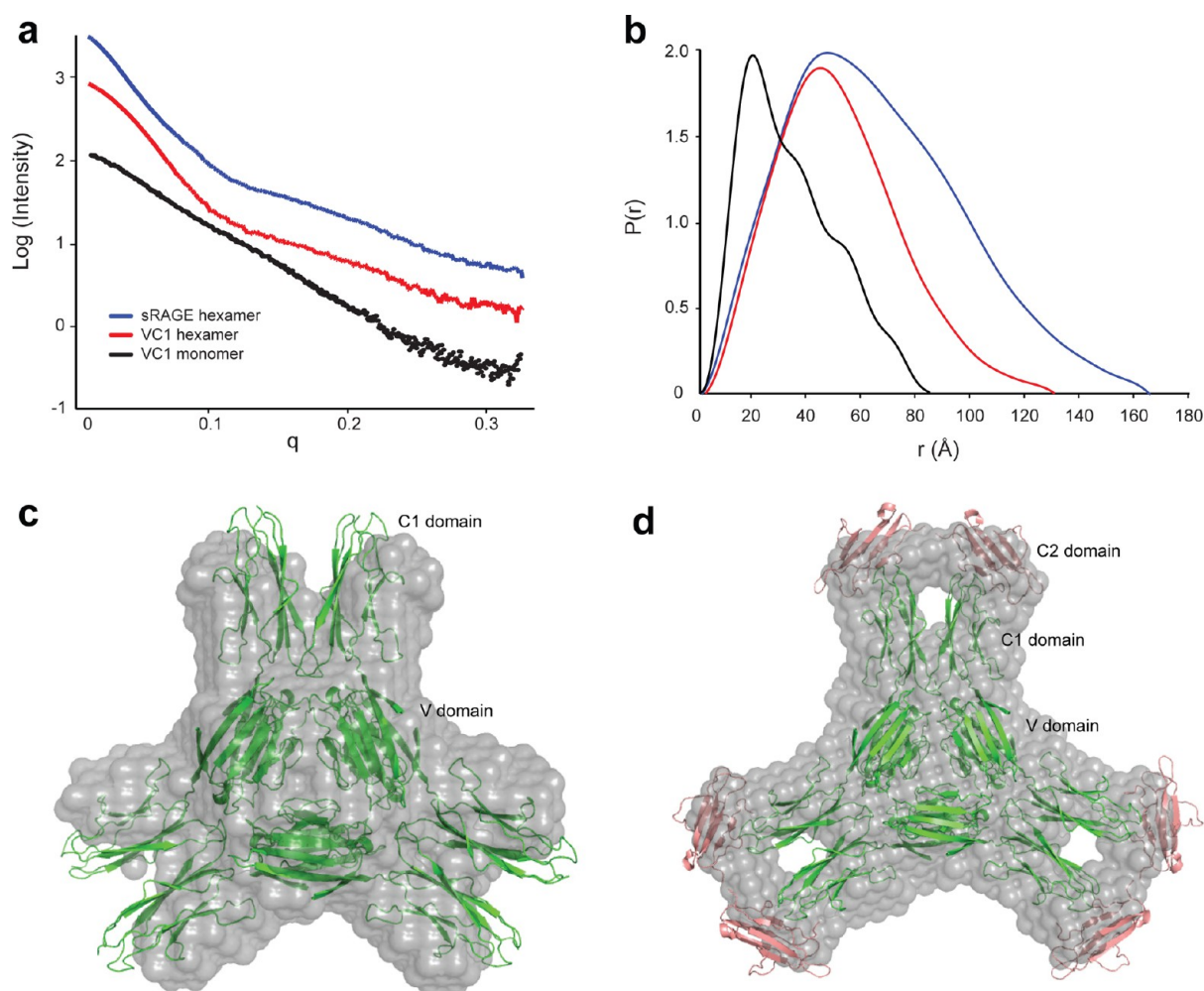
Figure 5. Solution structure of RAGE oligomer. (a) Raw SAXS scattering curves of the monomeric V-C1 domain, the hexameric V-C1 domain/dodecasaccharide complex and the hexameric sRAGE/dodecasaccharide complex. (b) $P(r)$ pair function analysis of the scattering curves. Profiles are colored as in panel a. (c) The GASBOR generated *ab initio* model of hexameric V-C1 is shown in gray and is superimposed on the crystal structure of V-C1 hexamer shown in green. (d) An *ab initio* model of hexameric sRAGE superimposed with the crystal structure of V-C1 hexamer (green) and the structure of C2 domain (PDB id: 2ENS, salmon) is shown.

The crystal structure shows clearly that the dimer is the basic building unit of the RAGE hexamer. The dimer possesses four discrete functional surfaces with almost no overlap. The flat ligand binding surfaces are located at the ends of the V domain. The hydrophobic dimerization interface is embedded centrally in the core of the dimer. The heparan sulfate-binding residues line a positive cleft between dimer-related subunits. The residues involved in interdimer interactions lie on the opposite side of the heparan sulfate-binding surface (Figure 3a and c). In the absence of heparin, RAGE does not dimerize in solution, suggesting that the hydrophobic interactions at the dimer interface must be too weak to sustain a dimer without an additional stabilizing factor. The small hydrophobic dimer interface is only 300 Å^2, much less than the 1200−2000 Å^2 interface commonly found at protein−protein interfaces.[26] Our mutational data indicates that hydrophobic and electrostatic interactions work synergistically to stabilize the dimer interface.

SAXS Analysis of RAGE Hexamer in Solution. The technique of small-angle X-ray scattering was used to assess whether the structure observed in the crystalline state is retained in solution. The scattering profile, $I(q)$, of V-C1 and the V-C1/oligosaccharide complex and the sRAGE/oligosaccharide complex reveals well-folded architecture, since plots of

$I(q)$ versus q reveal the fine structure expected for relatively fixed spatial arrangements of domains (Figure 5a).[27,28] The distance distribution function, $P(r)$, and Guinier plot was determined for all three data sets, from which real space R_G values were extracted (Figure 5b and Supplemental Table 4). MW estimations of the complexes based on scattering curves are also consistent with hexamer (Supplemental Table 4).

The theoretical scattering curve back-calculated from the crystal structure of hexameric V-C1 domain displays good agreement with the experimental scattering curve with a value of 2.5 for the Chi fitting parameter (Supplemental Figure 6). The experimental and simulated curves exhibit excellent overlap up until $q = 0.1$, which suggests the two structures have similar overall shape but that the average conformation in solution is different from the crystal structure. This observation is consistent with isolation of a specific low-energy conformation in the crystal from the ensemble of structures that are populated in solution.

We further generated low-resolution models of the complexes using the ab initio envelope reconstruction program GASBOR. The average GASBOR model of multiple runs based on $P3$ symmetry is presented in Figure 5c (V-C1 complex) and 5d (sRAGE complex). The overall shape of the V-C1 hexamer
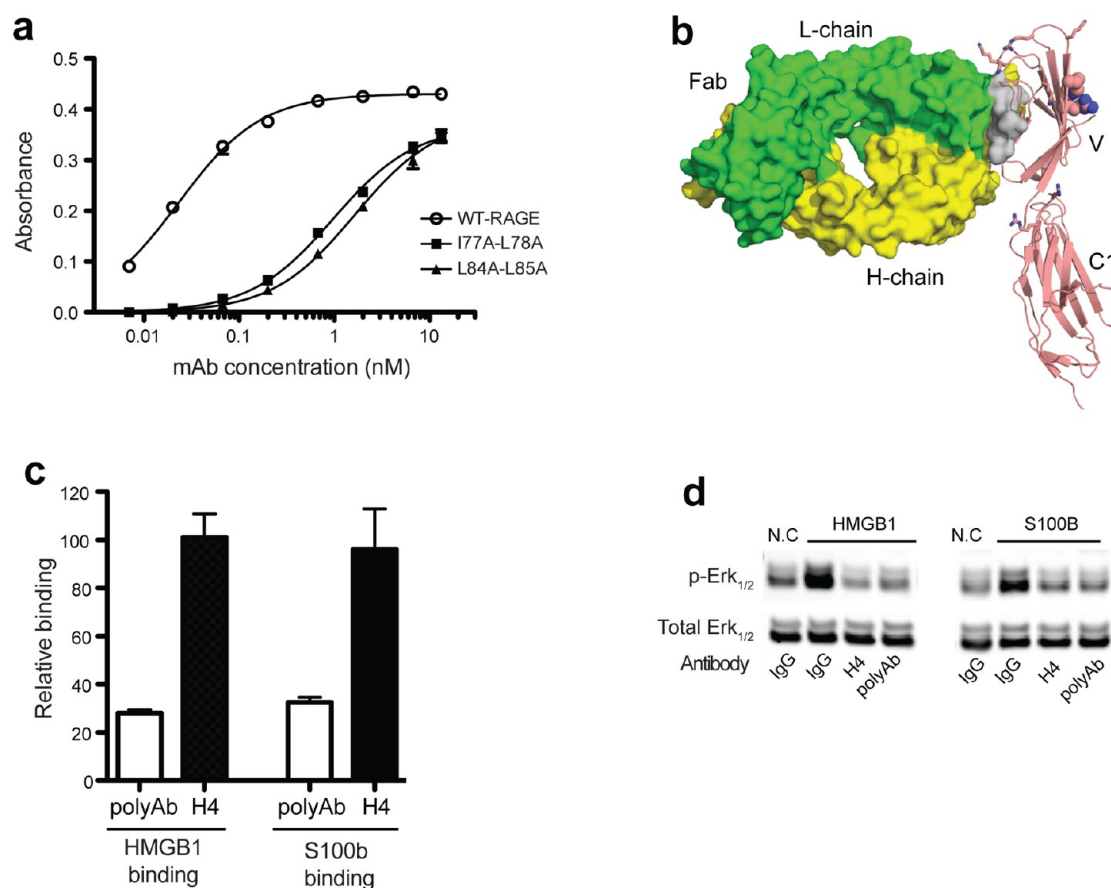
Figure 6. Targeting the oligomerization interface with a mAb blocks RAGE signaling. (a) Binding of anti-RAGE rabbit mAb H4 to immobilized wild-type mRAGE V-C1 domain, I77A-L78A (mouse equivalent of human V78A-L79A), and L84A-L85A (mouse equivalent of human F85A-L86A) mutants was determined by ELISA. (b) Postulated binding model of H4 to RAGE. Fab fragment (PDB id: 3GRW) of IgG is shown as surface representation with light chain in green and heavy chain in yellow. V-C1 is shown as cartoon in salmon. Also shown are the hydrophobic dimerization interface (gray surface), heparan sulfate binding residues (sticks) and ligand binding residues (spheres). (c) Binding of biotinylated mRAGE V-C1 domain to immobilized HMGB1 or S100b was measured in the absence or presence of anti-RAGE rabbit polyclonal Ab (polyAb) or H4 (both at 5 μg/mL). The percentage of inhibition was determined by comparing the absorbance value to standard binding curves of mRAGE V-C1 to HMGB1 or S100b. $n = 3$, the error bar represents SD. (d) Immunoblot analysis of $Erk_{1/2}$ and $phosphoErk_{1/2}$ in human endothelial cells after stimulation with HMGB1 or S100b. Cells were preincubated with nonspecific rabbit IgG, H4, or anti-RAGE polyAb at 5 μg/mL for 30 min prior to stimulation.

model bears striking similarity to our crystal structure, most notably the discrete representation of the six spokes that correspond to the C1 domains. Alignment of the GASBOR envelope of V-C1 hexamer to the crystal structure using SUPCOM showed a high degree of agreement ($\rho_f = 1.02$, Figure 5c). The GASBOR envelope of the sRAGE hexamer closely resembles that of the V-C1 hexamer, except that additional density is visible at the tip of the spokes. This additional volume nicely accommodates the C2 domains as shown in Figure 5d.

The combined results of the SAXS and crystallographic studies reveal that RAGE exists as a hexamer in the presence of heparan sulfate. This configuration resembles a wheel-like structure with the V domains forming the central hub, the C1 domains forming the spokes of the wheel, and the C2 domains forming a rim at the periphery. Although we lack conclusive evidence for oligosaccharide binding in the crystal, the lack of crystal formation in the absence of dodecasaccharide (under identical crystallization conditions) and positive difference-electron density in solvent channels of the crystal suggests the presence of heparin.

Our structural characterization of RAGE oligomerization provides insight relevant to how RAGE transduces signals across the cell membrane. Our data indicate that the RAGE hexamer lies parallel to the cell surface, with one or more heparan sulfate chains arrayed around the perimeter. In this orientation, the ligand-binding residues on the V domain (K52, R98 and K110) are fully exposed and would be available for ligand binding. It was reported that S100b interacts with this basic surface by electrostatic interactions possibly through a negatively charged surface.[10] In addition, S100b forms oligomers, and an octamer structure of S100b has been reported.[12] Interestingly, the diameter of the octameric S100b matches quite well to the center hub formed by the V domains (Supplemental Figure 7), suggesting that S100b could interact with RAGE in a multivalent manner. This orientation would also allow the C2 domains, which are connected to V-C1 through a flexible loop, and the transmembrane domains to orient perpendicular to the hexamer. We propose that such arrangement poises RAGE in a functionally ready state for signaling.

RAGE is an example of a growing number of receptors that depend on heparan sulfate for activity, which includes fibroblast

growth factor (FGF) and vascular endothelial growth factor (VEGF) receptors. Although RAGE bears many structural similarities to these receptors, it is unique in that the formation of RAGE hexamer depends only on heparan sulfate and exists in the absence of ligand, whereas the functional forms of FGF and VEGF receptors depend on ligand-induced dimerization and association with heparan sulfate.[29−32] These differences highlight the versatility of the heparan sulfate in regulating receptor activation. Notably, our study stresses that heparan sulfate can function entirely at the receptor level, without having to directly interact with its cognate ligands. Historically most heparan sulfate-binding receptors were discovered only after their heparan sulfate-binding ligands were known. We now need to reexamine the possibility that many more receptors exist that depend on direct interaction with heparan sulfate for activity.

Targeting RAGE Oligomerization with mAbs. Our characterization of the receptor complex suggested that disrupting RAGE oligomerization might block RAGE signaling. In fact, this mode of inhibition might be a more universal way to block RAGE signaling because it should affect signaling by most if not all RAGE ligands. To test this hypothesis, we generated a collection of rabbit mAbs against mouse RAGE V-C1 domain. Ninety mAbs were identified and mapped against the various mutants of RAGE, which led to the identification of one mAb (H4) that specifically targets the hydrophobic interface. Binding of H4 to RAGE depends on amino acid residues I77, L78, L84 and L85 (mouse homologues of human V78, L79, F85 and L86). Double mutants involving these residues showed 50- to 70-fold reduction in affinity of the mAb−RAGE interaction (Figure 6a), which suggests that H4 most likely directly targets the hydrophobic dimerization interface (a schematic view of the postulated H4:RAGE interaction is shown in Figure 6b). mAb H4 has an extremely high affinity for mouse RAGE with a K_d of 23 pM and cross-reacts with human RAGE with a K_d of 0.9 nM. As predicted, binding of mAb H4 to RAGE did not interfere with ligand binding (consistent with the location of the ligand binding site on the opposite side of the V domain; Figure 6b), whereas a rabbit polyclonal antibody substantially inhibited both HMGB1 and S100b binding (Figure 6c). These properties allowed us to directly test the effect of blocking RAGE oligomerization on RAGE signaling. When primary human endothelial cells were stimulated with either HMGB1 or S100b in the presence of mAb H4 at 5 μg/mL, $ERK_{1/2}$ phosphorylation was completely abolished (Figure 6d). The inhibition of signaling by this oligomerization-specific mAb suggests that RAGE oligomerization is an important part of signaling. Pharmaceutical inhibition of RAGE oligomerization might therefore be a feasible approach for inhibition of RAGE signaling in pathological conditions.

Most receptors require oligomerization for activity, suggesting that drug-like compounds or mAbs that target subunit interfaces could be a viable strategy for therapeutic intervention. Indeed, several tumor suppressing mAbs (Cetuximab and Matuzumab) abrogate EGF receptor signaling by preventing receptor dimerization.[33,34] Similarly, a mAb that inhibits FGFR3 dimerization has proven effective in inhibiting FGFR3 signaling in several tumor models.[35] Our development of an inhibitory mAb targeted to the dimer interface represents another example of effective targeting of receptor oligomerization. Theoretically, mAbs that specifically interfere with heparan sulfate binding would achieve the same effect by inhibiting formation of RAGE hexamers. Our success with this strategy might serve as a paradigm for developing mAbs to target other heparan sulfate-binding proteins that depend on heparan sulfate for oligomerization. Moreover, our experience with the dimer interface-specific mAb strongly suggests that the oligomerization interface could be explored as a target for computer-based virtual screening and drug design.

■ METHODS

Protein Expression. The production of recombinant sRAGE and site-directed mutagenesis are described in Supplemental Methods.

Immunoblotting. Human dermal microvascular endothelial cells (HDMVEC, Lonza) were serum starved in DMEM for 5 h prior to treatment with HMGB1 (50 ng/mL),[20] S100A8/A9 or S100A12 (5 μg/mL, gifts from Geetha Srikrishna), bovine S100b or AGE-BSA (5 μg/mL, EMD Biosciences). Selected samples were pretreated with heparin lyases as described.[20] Cells were lysed and resolved by SDS-PAGE and blotted with antibodies to $Erk_{1/2}$ and phospho-$Erk_{1/2}$ (Cell Signaling). Bands were visualized on an Odyssey Infrared imaging system (Li-Cor).

Analytical Size Exclusion Chromatography (SEC). Purified sRAGE monomer (100−200 μg) and size-defined heparin-derived oligosaccharides (Iduron) were incubated in 20 mM Tris, 200 mM NaCl, pH 7.7 at RT overnight. The complexes were resolved on a Superdex 200 SEC column (size 10/300 mm or 10/420 mm, GE Healthcare) or a SRT SEC-300 HPLC column (7.8/300 mm, Sepax). Disaccharide analysis provided by Iduron states that the trisulfated disaccharide (I2S6) represents about 75% of the disaccharides in the dodecasaccharide. The rest of the disaccharide species are mostly disulfated (I0S6 or I2S0). The method for SEC-MALS is described in Supplemental Methods.

Isothermal Titration Calorimetry (ITC). ITC was performed on a MicroCal VP-ITC at 25 °C. Titrations were performed by injecting 10 μL (for a total of 28 injections) of 60 or 80 μM dodecasaccharide into 10 μM protein in the sample cells. Both solutions were dialyzed into 20 mM Tris, 150 mM NaCl at pH 7.7 prior to the experiment. Data were analyzed using Origin software (5.0) assuming single-site binding.

Heparin-Sepharose Chromatography. Purified RAGE mutants (200 μg) were applied to a 1-mL HiTrap heparin-Sepharose column (GE Healthcare) and eluted with a salt gradient from 150 mM to 1 M NaCl at pH 7.2 (HEPES buffer). The conductivity measurements at the peak of the elution were converted to the concentration of NaCl.

Nitrocellulous Filter Binding Assay. Recombinant wild-type sRAGE or mutants (500 ng) were incubated with 10,000 counts of ^{35}S-labeled microvascular endothelial lung heparan sulfate in 100 μL of PBS for 1 h at 22 °C. The mixtures were applied to a prewashed nitrocellulose membrane in a Bio-Rad 96-well blot apparatus and washed with 100 μL of PBS twice. Free [35S]heparan sulfate passed through the membrane, and only the portions that bound to protein were retained. The membrane was eluted with 0.5 mL of HEPES buffer containing 1 M NaCl. Released [35S]heparan sulfate was measured by liquid scintillation counting. The extent of binding was quantified by dividing the counts retained by the membrane by the total input counts.

X-ray Crystallography. Mouse RAGE V-C1/dodecaccharide complex was concentrated to 10.25 mg mL^{-1} in 20 mM Tris, 100 mM NaCl, at pH 7.7. Crystals were obtained by vapor diffusion using the hanging drop method by mixing 2.0 μL of the complex with 2.0 μL of 0.1 M Tris pH 8.5, 200 mM $MgCl_2$, and 22% PEG 400. For data collection crystals were flash frozen in liquid nitrogen and placed into a stream of liquid nitrogen gas cooled to −180 °C. Diffraction data were collected to 3.5 Å on the Southeast Regional Collaborative Access Team 22-ID beamline at the Advanced Photon Source, Argonne National Laboratory. The structure was determined by molecular replacement in Phenix with the hRAGEV1C1 domain (PDB id: 3CJJ) as the starting model.[36] Refinement and model building were carried out using Phenix and COOT, respectively.[36,37]

SAXS Data Acquisition. Scattering data were collected at the beamline 12.3.1 at the Lawrence Berkeley National Laboratory. Monodisperse sRAGE/dodecasaccharide and V-C1/dodecasaccharide complexes purified by SEC were concentrated to 1, 3, and 6 mg mL^{-1} in a buffer containing 20 mM Tris, 200 mM NaCl, 1% glycerol at pH 7.7. The scattering profile of each sample was collected with 3 exposures (0.5, 1, and 6 s). SAXs data analysis is described in Supplemental Methods.

Rabbit Monoclonal Antibody (mAb). Rabbits were immunized with mouse RAGE V-C1 domain. After the desired titer was obtained, the antiserum was purified by immobilized RAGE to obtain the polyclonal anti-RAGE IgG. Splenocytes derived from the rabbits were fused with rabbit plasmacytoma cells 240E-W2 at Epitomics Inc. We screened 4,000 clones and obtained 90 positive clones by antigen binding ELISA (Supplemental Methods). Positive clones were subjected to epitope mapping by direct ELISA using immobilized heparan sulfate-binding mutants and dimerization mutants of RAGE. Mutants that showed reduced binding affinity to a given mAb compared to the wild-type RAGE defined residues that are part of the epitope. Rabbit mAb H4, which blocks the oligomerization of RAGE, was purified by Protein A chromatography from hybridoma supernatant.

ASSOCIATED CONTENT

Ⓢ Supporting Information

This material is available free of charge via the Internet at http://pubs.acs.org.

Accession Codes

Coordinates for the RAGE V-C1/dodecaccharide complex structure have been deposited with the Protein Data Bank under the accession code 4IM8.

AUTHOR INFORMATION

Corresponding Author
*E-mail: dxu@ucsd.edu; jesko@ucsd.edu.

Author Contributions
D.X., L.P., W.J.C. and J.D.E. designed the research; D.X., L.P., J.Y. and D.S performed the work and statistical analyses; D.X., L.P., J.Y., D.S., W.J.C., K.C., J.K. and J.D.E. analyzed and interpreted data; and D.X., W.J.C., L.P. and J.D.E. wrote the manuscript.

Notes
The authors declare no competing financial interest.

REFERENCES

(1) Brownlee, M., Cerami, A., and Vlassara, H. (1988) Advanced glycosylation end products in tissue and the biochemical basis of diabetic complications. *N. Engl. J. Med. 318*, 1315−1321.

(2) Basta, G. (2008) Receptor for advanced glycation endproducts and atherosclerosis: From basic mechanisms to clinical implications. *Atherosclerosis 196*, 9−21.

(3) Sims, G. P., Rowe, D. C., Rietdijk, S. T., Herbst, R., and Coyle, A. J. (2010) HMGB1 and RAGE in inflammation and cancer. *Annu. Rev. Immunol. 28*, 367−388.

(4) Liliensiek, B., Weigand, M. A., Bierhaus, A., Nicklas, W., Kasper, M., Hofer, S., Plachky, J., Grone, H. J., Kurschus, F. C., Schmidt, A. M., Yan, S. D., Martin, E., Schleicher, E., Stern, D. M., Hammerling, G. G., Nawroth, P. P., and Arnold, B. (2004) Receptor for advanced glycation end products (RAGE) regulates sepsis but not the adaptive immune response. *J. Clin. Invest. 113*, 1641−1650.

(5) Muhammad, S., Barakat, W., Stoyanov, S., Murikinati, S., Yang, H., Tracey, K. J., Bendszus, M., Rossetti, G., Nawroth, P. P., Bierhaus, A., and Schwaninger, M. (2008) The HMGB1 receptor RAGE mediates ischemic brain damage. *J. Neurosci. 28*, 12023−12031.

(6) Park, L., Raman, K. G., Lee, K. J., Lu, Y., Ferran, L. J., Jr., Chow, W. S., Stern, D., and Schmidt, A. M. (1998) Suppression of accelerated diabetic atherosclerosis by the soluble receptor for advanced glycation endproducts. *Nat. Med. 4*, 1025−1031.

(7) Yan, S. F., Ramasamy, R., and Schmidt, A. M. (2010) The RAGE axis: a fundamental mechanism signaling danger to the vulnerable vasculature. *Circ. Res. 106*, 842−853.

(8) Yan, S. S., Wu, Z. Y., Zhang, H. P., Furtado, G., Chen, X., Yan, S. F., Schmidt, A. M., Brown, C., Stern, A., LaFaille, J., Chess, L., Stern, D. M., and Jiang, H. (2003) Suppression of experimental autoimmune encephalomyelitis by selective blockade of encephalitogenic T-cell infiltration of the central nervous system. *Nat. Med. 9*, 287−293.

(9) Dattilo, B. M., Fritz, G., Leclerc, E., Kooi, C. W., Heizmann, C. W., and Chazin, W. J. (2007) The extracellular region of the receptor for advanced glycation end products is composed of two independent structural units. *Biochemistry 46*, 6957−6970.

(10) Koch, M., Chitayat, S., Dattilo, B. M., Schiefner, A., Diez, J., Chazin, W. J., and Fritz, G. (2010) Structural basis for ligand recognition and activation of RAGE. *Structure 18*, 1342−1352.

(11) Leclerc, E., Fritz, G., Weibel, M., Heizmann, C. W., and Galichet, A. (2007) S100B and S100A6 differentially modulate cell survival by interacting with distinct RAGE (receptor for advanced glycation end products) immunoglobulin domains. *J. Biol. Chem. 282*, 31317−31331.

(12) Ostendorp, T., Leclerc, E., Galichet, A., Koch, M., Demling, N., Weigle, B., Heizmann, C. W., Kroneck, P. M., and Fritz, G. (2007) Structural and functional insights into RAGE activation by multimeric S100B. *EMBO J. 26*, 3868−3878.

(13) Xue, J., Rai, V., Singer, D., Chabierski, S., Xie, J., Reverdatto, S., Burz, D. S., Schmidt, A. M., Hoffmann, R., and Shekhtman, A. (2011) Advanced glycation end product recognition by the receptor for AGEs. *Structure 19*, 722−732.

(14) Sakaguchi, M., Murata, H., Yamamoto, K., Ono, T., Sakaguchi, Y., Motoyama, A., Hibino, T., Kataoka, K., and Huh, N. H. (2011) TIRAP, an adaptor protein for TLR2/4, transduces a signal from RAGE phosphorylated upon ligand binding. *PLoS One 6*, e23132.

(15) Hudson, B. I., Kalea, A. Z., Del Mar Arriero, M., Harja, E., Boulanger, E., D'Agati, V., and Schmidt, A. M. (2008) Interaction of the RAGE cytoplasmic domain with diaphanous-1 is required for ligand-stimulated cellular migration through activation of Rac1 and Cdc42. *J. Biol. Chem. 283*, 34457−34468.

(16) Ishihara, K., Tsutsumi, K., Kawane, S., Nakajima, M., and Kasaoka, T. (2003) The receptor for advanced glycation end-products (RAGE) directly binds to ERK by a D-domain-like docking site. *FEBS Lett. 550*, 107−113.

(17) Xie, J., Reverdatto, S., Frolov, A., Hoffmann, R., Burz, D. S., and Shekhtman, A. (2008) Structural basis for pattern recognition by the receptor for advanced glycation end products (RAGE). *J. Biol. Chem. 283*, 27255−27269.

(18) Zong, H., Madden, A., Ward, M., Mooney, M. H., Elliott, C. T., and Stitt, A. W. (2010) Homodimerization is essential for the receptor for advanced glycation end products (RAGE)-mediated signal transduction. *J. Biol. Chem.* 285, 23137−23146.

(19) Sarkany, Z., Ikonen, T. P., Ferreira-da-Silva, F., Saraiva, M. J., Svergun, D., and Damas, A. M. (2011) Solution structure of the soluble receptor for advanced glycation end products (sRAGE). *J. Biol. Chem.* 286, 37525−37534.

(20) Xu, D., Young, J., Song, D., and Esko, J. D. (2011) Heparan sulfate is essential for High Mobility Group Protein 1 (HMGB1) signaling by the Receptor for Advanced Glycation End Products (RAGE). *J. Biol. Chem.* 286, 41736−41744.

(21) Goyette, J., Yan, W. X., Yamen, E., Chung, Y. M., Lim, S. Y., Hsu, K., Rahimi, F., Di Girolamo, N., Song, C., Jessup, W., Kockx, M., Bobryshev, Y. V., Ben Freedman, S., and Geczy, C. L. (2009) Pleiotropic roles of S100A12 in coronary atherosclerotic plaque formation and rupture. *J Immunol.* 183, 593−603.

(22) Robinson, M. J., Tessier, P., Poulsom, R., and Hogg, N. (2002) The S100 family heterodimer, MRP-8/14, binds with high affinity to heparin and heparan sulfate glycosaminoglycans on endothelial cells. *J. Biol. Chem.* 277, 3658−3665.

(23) Hofmann, M. A., Drury, S., Fu, C., Qu, W., Taguchi, A., Lu, Y., Avila, C., Kambham, N., Bierhaus, A., Nawroth, P., Neurath, M. F., Slattery, T., Beach, D., McClary, J., Nagashima, M., Morser, J., Stern, D., and Schmidt, A. M. (1999) RAGE mediates a novel proinflammatory axis: a central cell surface receptor for S100/calgranulin polypeptides. *Cell* 97, 889−901.

(24) Rai, V., Toure, F., Chitayat, S., Pei, R., Song, F., Li, Q., Zhang, J., Rosario, R., Ramasamy, R., Chazin, W. J., and Schmidt, A. M. (2012) Lysophosphatidic acid targets vascular and oncogenic pathways via RAGE signaling. *J. Exp. Med.* 209, 2339−2350.

(25) Park, H., Adsit, F. G., and Boyington, J. C. (2010) The 1.5 Å crystal structure of human receptor for advanced glycation end-products (RAGE) ectodomains reveals unique features determining ligand binding. *J. Biol. Chem.* 285, 40762−40770.

(26) Janin, J., Bahadur, R. P., and Chakrabarti, P. (2008) Protein-protein interaction and quaternary structure. *Q. Rev. Biophys.* 41, 133−180.

(27) Bernado, P. (2010) Effect of interdomain dynamics on the structure determination of modular proteins by small-angle scattering. *Eur. Biophys. J.* 39, 769−780.

(28) Heller, W. T. (2005) Influence of multiple well defined conformations on small-angle scattering of proteins in solution. *Acta Crystallogr., Sect. D: Biol. Crystallogr.* 61, 33−44.

(29) Mohammadi, M., Olsen, S. K., and Ibrahimi, O. A. (2005) Structural basis for fibroblast growth factor receptor activation. *Cytokine Growth Factor Rev.* 16, 107−137.

(30) Schlessinger, J., Plotnikov, A. N., Ibrahimi, O. A., Eliseenkova, A. V., Yeh, B. K., Yayon, A., Linhardt, R. J., and Mohammadi, M. (2000) Crystal structure of a ternary FGF-FGFR-heparin complex reveals a dual role for heparin in FGFR binding and dimerization. *Mol. Cell* 6, 743−750.

(31) Brozzo, M. S., Bjelic, S., Kisko, K., Schleier, T., Leppanen, V. M., Alitalo, K., Winkler, F. K., and Ballmer-Hofer, K. (2012) Thermodynamic and structural description of allosterically regulated VEGFR-2 dimerization. *Blood* 119, 1781−1788.

(32) Xu, D., Fuster, M. M., Lawrence, R., and Esko, J. D. (2011) Heparan sulfate regulates VEGF165- and VEGF121-mediated vascular hyperpermeability. *J. Biol. Chem.* 286, 737−745.

(33) Leahy, D. J. (2008) A molecular view of anti-ErbB monoclonal antibody therapy. *Cancer Cell* 13, 291−293.

(34) Schmiedel, J., Blaukat, A., Li, S., Knochel, T., and Ferguson, K. M. (2008) Matuzumab binding to EGFR prevents the conformational rearrangement required for dimerization. *Cancer Cell* 13, 365−373.

(35) Qing, J., Du, X., Chen, Y., Chan, P., Li, H., Wu, P., Marsters, S., Stawicki, S., Tien, J., Totpal, K., Ross, S., Stinson, S., Dornan, D., French, D., Wang, Q. R., Stephan, J. P., Wu, Y., Wiesmann, C., and Ashkenazi, A. (2009) Antibody-based targeting of FGFR3 in bladder carcinoma and t(4;14)-positive multiple myeloma in mice. *J. Clin. Invest.* 119, 1216−1229.

(36) Zwart, P. H., Afonine, P. V., Grosse-Kunstleve, R. W., Hung, L. W., Ioerger, T. R., McCoy, A. J., McKee, E., Moriarty, N. W., Read, R. J., Sacchettini, J. C., Sauter, N. K., Storoni, L. C., Terwilliger, T. C., and Adams, P. D. (2008) Automated structure solution with the PHENIX suite. *Methods Mol. Biol.* 426, 419−435.

(37) Emsley, P., and Cowtan, K. (2004) Coot: model-building tools for molecular graphics. *Acta Crystallogr., Sect. D: Biol. Crystallogr.* 60, 2126−2132.